Mid-Infrared Ellipsometry, Raman and X-ray Diffraction Studies of $Al_xGa_{1-x}N/AlN/Si$ Structures

Chennan Wang[1], Ondřej Caha[1], Filip Münz[1], Petr Kostelník[2], Tomáš Novák[2], and Josef Humlíček[1]

1. Masaryk University, Department of Condensed Matter Physics and CEITEC - Central European Institute of Technology, Kotlářská 2, 61137 Brno, Czech Republic

2. ON Semiconductor Czech Republic, 1. máje 2230, 756 61 Rožnov pod Radhoštěm, Czech Republic

Abstract

We report an investigation of the optical and structural properties of wurtzite phase $Al_xGa_{1-x}N/AlN$ structure grown on Si(111) within the compositional range of $0 \leq x \leq 1$. The study focuses on providing essential physical quantities for the fabrication process control, namely the composition dependence of phonon mode energy and refractive index. Three complementary techniques, infrared ellipsometry, Raman spectroscopy and X-ray diffraction, have been used to minimize the uncertainty in our analysis. Based on the high quality and nearly strain-free $Al_xGa_{1-x}N/AlN$ double layer samples, we determined the calibration curve for the A_1(LO) phonon mode. We have also constructed the ellipsometry model which uses *a-priori* knowledge of experimentally measured A_1(TO) phonon mode frequencies. From the best model fit to the collected ellipsometry spectra of the entire sample series, we obtained the anisotropic refractive indices of the $Al_xGa_{1-x}N$ alloys with a very satisfactory accuracy.

I. Introduction

The group III nitrides and their heterostructures are technologically important in optoelectric, high power and high frequency electronic devices, owing to the materials' wide tunable bandgap [1] and the ability of formation a two-dimensional electron gas with high sheet charge carrier density [2]. The fabrication of group III nitride device can use sapphire, silicon-carbide or silicon substrates [3]. Among which, silicon substrate attracts considerable attention due to the potential of bringing down the fabrication cost, by using less expensive material and boosting the production volume with large diameter wafers.

The well known obstacle in fabrication of high-quality layers is the lattice mismatch between the nitrides and the silicon substrate, as well as the difference in their thermal expansion coefficients. The problem causes phase separation and high defect density in the epitaxial layers, which makes the quality of the GaN epitaxial layer by direct growth on silicon far from satisfactory. In order to overcome this problem, an alternative approach of introducing an interlayer, like (HT)AlN-Si [4], (LT)AlN-(HT)AlN-Si [5],

$Al_xGa_{1-x}N$ step-graded layer [6], $Al_xGa_{1-x}N$ composition graded layer [7], have shown improved GaN layer quality due to the released strain above the interlayer.

In this paper, we focus on evaluating the high-quality wurtzite $Al_xGa_{1-x}N/AlN$ heterostructures grown on silicon (111) surface. By combining mid-infrared (MIR) ellipsometry with Raman spectroscopy and X-ray diffraction (XRD) techniques, we address the extraction of important parameters of the nitride layered structures, aimed at providing information for optimization of $Al_xGa_{1-x}N$ on silicon epitaxial technology. We firstly present the results of XRD measurement, identifying the composition and the strain of the nitride layers. Then, we report on Raman spectroscopic analysis aiming at the compositional characterization of the $Al_xGa_{1-x}N$ alloy, the retrieved phonon frequencies provide essential reference for modeling ellipsometric spectra. Finally, we perform a spectroscopic ellipsometric analysis of the layered samples in the whole compositional range of the $Al_xGa_{1-x}N$ alloys. Using the anisotropic multilayer model, we have achieved good agreement between the measured and modeled ellipsometric data. The determined dielectric function of each layer provides essential reference for further optimization of the $Al_xGa_{1-x}N/Si$ fabrication process.

II. Samples and Experimental Methods

The samples used in our research were provided by ON Semiconductor company. The wurtzite phase $Al_xGa_{1-x}N/AlN$ double layers were grown by Metalorganic Chemical Vapour Deposition (MOCVD) method in a commercial reactor Veeco TurboDisc K465i on undoped Si(111) wafers. Hydrogen and nitrogen were used as the carrier gases and ammonia, trimethylgallium and trimethylalluminium as the source materials. Each sample consists of a thin AlN nucleation layer followed by a thicker $Al_xGa_{1-x}N$ alloy layer. The typical thickness of the AlN buffer layer is about 200 nm. But the upper AlGaN layer with nominal thickness 800 nm has a little bit higher spread within our sample series. The top layer covers a broad Al compositional range from 0 to 0.85. The deposition conditions (substrate temperature, pressure, precursor flow, deposition rate) were subject to optimization, resulting in substantial variations of relevant parameters. A sample with a single nucleation layer on silicon substrate has also been provided as a reference.

The X-ray experiments were performed using Rigaku Smartlab diffractometer. We have used a parabolic multilayer mirror as a collimator, a germanium 2×220 channel-cut monochromator and a linear position sensitive detector. For the hexagonal wurtzite structure of $Al_xGa_{1-x}N$ alloy, the position of the diffraction

peak in reciprocal space (Q_x, Q_z) can be calculated by following formulas:

$$Q_z = \frac{2\pi}{l}c, \quad \text{and} \quad Q_x = \frac{4\pi}{a\sqrt{3}}\sqrt{h^2 + k^2 + m^2}. \tag{1}$$

We have assumed that $Al_xGa_{1-x}N$ obey the linear Vegard's law dependence of both lattice parameters on the Al concentration x according to Refs.[8, 9, 10]:

$$a(x) = (1-x)a_{\mathrm{GaN}} + xa_{\mathrm{AlN}}, \quad \text{and} \quad c(x) = (1-x)c_{\mathrm{GaN}} + xc_{\mathrm{AlN}}. \tag{2}$$

Since the surface of our samples is stress free, the in-plane and out-of-plane strain components are connected via Poisson ratio, which can be approximated by the value of $\nu = 0.26$ for whole composition range [11, 12],

$$2\nu \frac{a_{\mathrm{exp}} - a(x)}{a(x)} + \frac{c_{\mathrm{exp}} - c(x)}{c(x)} = 0. \tag{3}$$

Thus, the XRD measurements allow us to decouple composition and stress in each individiual layer of $Al_xGa_{1-x}N$ structure. The relative precision of the lattice parameters measurement is about 4×10^{-4}, which corresponds to the composition precision of $\delta x \approx 1\%$.

Raman spectra of the double layer samples were measured using a Renishaw InVia Raman microscope in backscattering configuration, with excitation laser wavelength of 633 nm. The circular spot on the sample has the diameter of about 1 μm. With the excitation energy in the visible range, the signal monitors the whole layered structure which is transparent for the entire Al composition level of the nitride alloys (GaN has the lowest bandgap energy among the series of alloys, about 3.4 eV at 300 K). Also, a strong signal from the silicon substrate is observed. The silicon peak has been used for the instrument calibration prior to each collection of the spectrum. The observed width of the peak is determined by the natural linewidth and instrumental resolution. For the main silicon peak, we typically achieve a full-width at half-maximum (FWHM) of 3.5-4.2 cm^{-1} at room temperature. Raman spectra provide information on lattice vibrations. The intensity of the Raman signal follows selection rules which are determined by the Raman tensor of the material and the polarization of the scattered electric field vector. Two scattering configurations of the Raman measurement have been used, namely $z(\text{-,-})\bar{z}$ and $x(\text{-,-})\bar{x}$ in Porto's notations, are collected from the top of the wafer center and from the side of cut wafers at the same place, respectively. The background signal of silicon have been subtracted. The spectral positions of Raman bands are of primary interest in determining the composition and assessing the quality of nitride layers and the stress due to the lattice mismatch [13]. The value of the phonon mode energy has been retrieved directly as its intensity maximum of the Raman lineshape, with the accuracy of ± 0.5 cm^{-1}. Using the two measurement configurations, we have obtained the A_1(LO) and A_1(TO), $E_{1,2}$(TO) frequencies in the

complete sample series.

Spectroscopic ellipsometry measurements were performed on a commercial ellipsometer (Woollam IR-VASE Mark I) in reflection geometry with the Polarizer-Sample-rotating Compensator (PSCr) configuration. The spectra were collected with a DTGS detector in the broad infrared range of 333 - 6200 cm^{-1}, with the spectrometer resolution setting of 4 cm^{-1}. For each wafer, two angles of incidence measurements were used, 60° and 75°. The relationship between the measured ellipsometric quantity $\tilde{\rho}$ and the Fresnel reflection coefficient $\tilde{r}$ is given by

$$\tilde{\rho} \equiv \frac{\tilde{r}_{\mathrm{p}}}{\tilde{r}_{\mathrm{s}}} = \frac{\sqrt{R_{\mathrm{p}}}}{\sqrt{R_{\mathrm{s}}}} \mathrm{e}^{\mathrm{i}(\delta\phi_{\mathrm{p}} - \delta\phi_{\mathrm{s}})} = \tan(\Psi)\mathrm{e}^{\mathrm{i}\Delta}. \tag{4}$$

The modeling of the ellipsometry data was done with the WVASE software. The model consists of the substrate, two uniaxial layers and a surface roughness layer at the top. The substrate has been described by a dispersion model provided by the software (si_ir.mat) [14]. The surface roughness of the top layer has been modeled using the Bruggeman effective medium approximation (B-EMA) bewteen the ambient and the top layer with equal volume fractions [15]. The epitaxial layers are uniaxially anisotropic with the optical axis oriented normal to the substrate surface. We have modeled the in-plane and the out-of-plane dielectric functions independently. The Fresnel reflection coefficients of p- and s- polarization states are given by:

$$\tilde{r}_{\mathrm{p}} \equiv \frac{\tilde{E}^{\mathrm{p}}_{\mathrm{ref}}}{\tilde{E}^{\mathrm{p}}_{\mathrm{inc}}} = \frac{\sqrt{1 - \dfrac{\sin^2\theta}{\tilde{\epsilon}_{\mathrm{e}}}} - \sqrt{\tilde{\epsilon}_{\mathrm{o}}}\cos\theta}{\sqrt{1 - \dfrac{\sin^2\theta}{\tilde{\epsilon}_{\mathrm{e}}}} + \sqrt{\tilde{\epsilon}_{\mathrm{o}}}\cos\theta} \quad \text{and} \quad \tilde{r}_{\mathrm{s}} \equiv \frac{\tilde{E}^{\mathrm{s}}_{\mathrm{ref}}}{\tilde{E}^{\mathrm{s}}_{\mathrm{inc}}} = \frac{\cos\theta - \sqrt{\tilde{\epsilon}_{\mathrm{o}} - \sin^2\theta}}{\cos\theta + \sqrt{\tilde{\epsilon}_{\mathrm{o}} - \sin^2\theta}}, \tag{5}$$

where θ is the angle of incidence, $\tilde{\epsilon}_{\mathrm{o}}$ and $\tilde{\epsilon}_{\mathrm{e}}$ are the in-plane (ordinary) and out-of-plane (extraordinary) dielectric function, respectively.

Along each direction, the transverse optical (TO) and longitudinal optical (LO) phonons are described using Lorentzian lineshapes [16], with their oscillator strength A, eigenfrequency ω and broadening γ determined by the fitting. It is worth to note that, the coupling between the TO-LO phonon pairs, especially at around 50%-50% mixture of the Al-Ga, will result an asymmetric lineshape of the E_1(TO) mode. Hence, we also have made the attempt to adopt the so-called 4-parameter TOLO model [17], which allows to access the LO frequency directly and adapts to the asymmetric phonon absorption profiles. However, in our trials, the advantage of the TOLO model for better describing the asymmetric phonon lineshapes was set back by the difficulty of finding the uniqueness of the fit due to the additional free parameters. Therefore, we resort to the harmonic oscillator approximation (HOA) approach which

using the symmetric Lorentizian to analyze our ellipsometry data. We find despite the E_1 (GaN like) mode is slightly asymmetric leading a fitting errorbar of determined phonon position about 5 cm^{-1}, the rest of the ellipsometric spectra is otherwise very well fitted.

The in-plane phonon mode E_1(TO) is known to follow the so-called "two-mode" behavior, which is due to the contrast in bond-lengths or mass difference in alloy mixtures [18, 19, 20]. Our model accounts for this phenomenon by using two independent Lorentz oscillators. For the out-of-plane phonon mode, the "two-mode" behavior is insignificant for the alloys with the Al content below 85% [21, 22]. A single mode is used in our analysis procedure to approximate the out-of-plane phonon contribution. It is important to point out that the ellipsometric measurement is not sensitive to the TO phonon modes along the out-of-plane direction (Eq. 5); we have therefore fixed their parameters using the values determined from the Raman experiments.

Dispersion in the transparent range due to the polar vibrations is contained in the used models while the electronic contribution is negligible due to the large bandgaps (above 3.4 eV). In addition, the high-frequency limit of the dielectric function, ϵ_∞, and the layer thickness are set to be free parameters in the fitting.

The dielectric functions of the epitaxial nitride layers have been obtained through the global fitting of the parameterized model to the measured ellipsometric quantities Ψ and Δ. The goodness of fit has been calculated using the Root Mean Square Deviation (RMSD) which is defined as:

$$\mathrm{RMSD} = \sqrt{\frac{1}{2N-M}\sum_{j=1}^{N}\left(\frac{\Psi_j^{\mathrm{mod}}-\Psi_j^{\mathrm{exp}}}{\varsigma_{\Psi,j}^{\mathrm{exp}}}\right)^2+\left(\frac{\Delta_j^{\mathrm{mod}}-\Delta_j^{\mathrm{exp}}}{\varsigma_{\Delta,j}^{\mathrm{exp}}}\right)^2}, \tag{6}$$

where N is the number of (Ψ, Δ) pairs, M is the number of variables in the model, and ς is the standard deviation of the experimental values.

III. Results and Interpretations

A. XRD

Reciprocal space maps were collected in the vicinity of three reciprocal lattice points (0002), (0004), and (11$\bar{2}$4) for all samples.

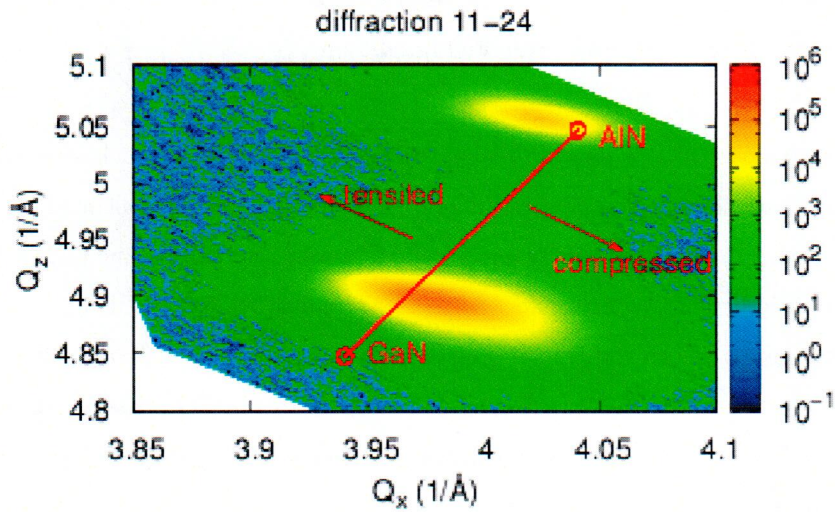

FIG. IIIA1 Reciprocal space map of x-ray scattered intensity in the vicinity of $11\bar{2}4$ reciprocal lattice point of $Al_{0.30}Ga_{0.70}N$/AlN/Si sample. Red line shows the position of the ideal unstrained $Al_xGa_{1-x}N$ peak. Left bottom and right top end of the line correspond to pure GaN and AlN lattice, respectively. Position of the diffraction peak along the red line is proportional to the chemical composition. The offset of the peak position from the red line is proportional to elastic strain as indicated by the arrows.

Figure IIIA1 shows the measured data at the lattice point ($11\bar{2}4$) of the Al=30% sample. Two diffraction peaks were observed for all samples, corresponding to the nucleation AlN layer and $Al_xGa_{1-x}N$ layer. From the peak position in the asymmetric $11\bar{2}4$ diffraction we have determined both a and c lattice parameters. The measured values were then used to evaluate chemical composition and strain of both AlN and $Al_xGa_{1-x}N$ layers. The results are summarized in the Tab. IIIA1.

	$Al_xGa_{1-x}N$		AlN	
Al(%)	ε_{xx}	ε_{zz}	ε_{xx}	ε_{zz}
0	0.002	-0.001	0.006	-0.004
5	0.001	-0.001	0.003	-0.002
11	0.001	-0.000	0.003	-0.002
19	0.001	-0.001	0.005	-0.003
30	-0.003	0.002	0.003	-0.002
42	-0.003	0.002	0.003	-0.002
49	0.000	0.000	0.003	-0.002
60	0.000	0.000	0.003	-0.002
71	0.000	-0.000	0.003	-0.002
79	0.000	-0.000	0.002	-0.001
85	0.002	-0.001	0.003	-0.002
100	0.004	-0.002	–	–

TAB. IIIA1 In-plane ε_{xx} and out-of-plane ε_{zz} strain components.

Apart from few samples, the Tab. IIIA1 indicates that the strain in the upper $Al_xGa_{1-x}N$ is very well relaxed. Two wafers (30 and 42% Al) had an upper layer only about 250 nm thick, hence we observed the higher strain in those samples as measured by X-ray diffraction. Furthermore, the evolution with the Al content is related to the variable growth conditions. The samples with low Al content have also a large lattice mismatch between the first and the second layer, resulting in a lower level of structural quality as seen in 0% and 5% Al content sample.

B. Raman

The spectral range of the out-of-plane longitudinal optical mode (LO) of A_1 symmetry (730-870 cm^{-1}) is of particular interest for the characterization purposes since it is accessible in the simple $z(\text{-},\text{-})\bar{z}$ backscattering configuration. Measured Raman lineshapes on a series of double-layer samples are shown in Fig. IIIB1. The spectra were obtained in the $z(\text{-},\text{-})\bar{z}$ backscattering geometry and the silicon contribution was subtracted.

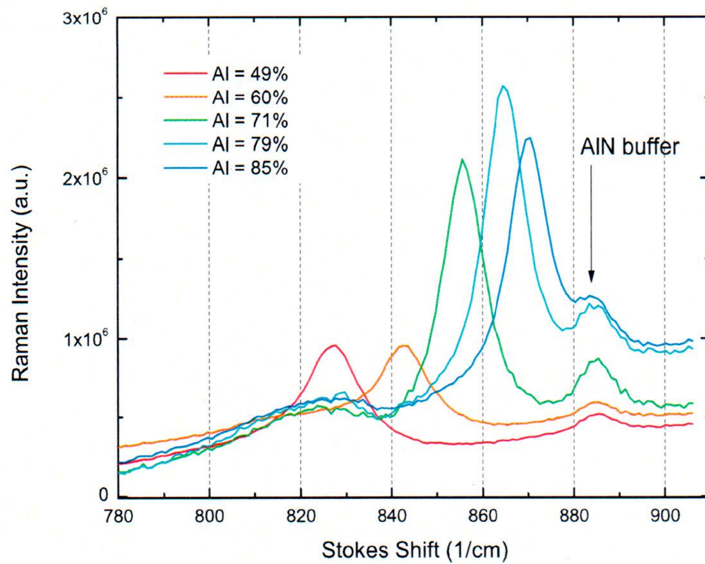

FIG. IIIB1 Raman spectra in $z(\text{-},\text{-})\bar{z}$ backscattering geometry. The Raman intensity is the difference between the nitride epitaxial layer and silicon substrate of each wafer. The strongest peak of each spectrum is at the A_1(LO) frequency of AlGaN alloys.

Evidently, the A_1(LO) modes are sensitive to the Al concentration but rather insensitive to the strain. From previous studies, the relationship between the mode energy and the Al concentration has been established [21, 23]. The position of Raman bands is in one-to-one correspondence with the composition and the strain in the film. Shown in Fig. IIIB2 is a summary of the A_1(LO) phonon frequency as a function of the Al concentration values deduced from our XRD measurements. The data are collected from different batches of samples with non-identical preparation conditions. Despite of the differences, the calibration curve presents an uniform trend. To find the necessary calibration curve for alloy compositions, a third-order polynomial is used for fitting the data, giving

$$\omega\ (1/\mathrm{cm}) = 734.3(12) + 2.74(10)x - 0.0203(23)x^2 + 0.000079(15)x^3, \tag{7}$$

with x in atomic percent. The standard deviation of the measured peak positions from the polynomial is about 1.2 cm^{-1}. Since the estimated uncertainty of Raman peak position is less than 0.5 cm^{-1}, the deviations are likely to be due to the uncertainties of the XRD results. Our value shows a good agreement with the data reported by Davydov et al.,[22].

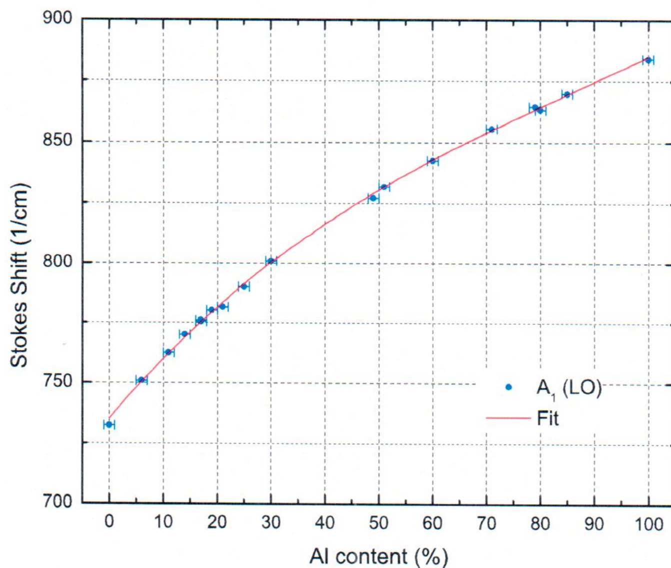

FIG. IIIB2 Summary of the A_1(LO) mode positions measured in $z(\text{-},\text{-})\bar{z}$ configuration as a function of Al content. The obtained calibration curve of A_1(LO) mode energy as a function of alloy composition is shown in red line.

Shown in Fig. IIIB3 are Raman spectra measured in $x(\text{-},\text{-})\bar{x}$ backscattering geometry. The transverse optical vibrations of A_1 mode also exhibit a strong dependence on the Al concentration. The mode energy can be easily determined since the A_1(TO) mode is well separated from the E(TO) symmetry modes which are identified as E_2(high) or a E_1(TO). For Al content > 30%, the positions of GaN-like modes of E_2(high) and E_1(TO) are almost coincide. The E2(high) frequency of AlN-like mode lies around 10 cm^{-1} below the E_1(TO) [22], hence lead a mixture of both peaks in our observed Raman spectra. A detailed description of the two modes will be addressed in our ellipsometry analysis.

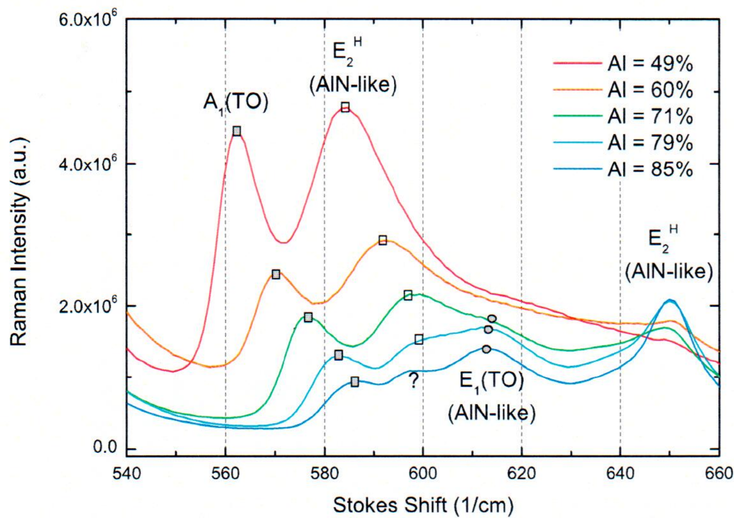

FIG. IIIB3 Measured Raman spectra on different alloy compositions in $x(\text{-,-})\bar{x}$ backscattering geometry. The positions of the A_1(TO) phonon mode along with other modes are marked with distinguishable symbols. For some remaining spectral features (marked with "?") we have no clear identification.

The A_1(TO) mode frequency of the whole series of samples is summarized in Fig. IIIB4. For comparison purposes, the strain of epitaxial layers along the z-axis direction is presented in the same graph. The XRD values demonstrate the majority of the $Al_xGa_{1-x}N$ layers are close to strain free, apart from the samples with Al composition around 30%-40%. The plot clearly demonstrates a correlation between the A_1(TO) mode energy and the out-of-plane lattice distortion. Note that, this effect is absent in the A_1(LO) modes.

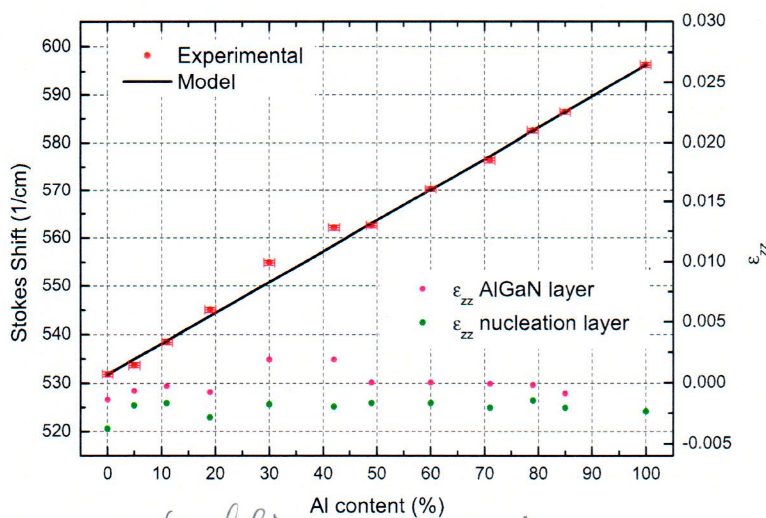

FIG. IIIB4 A_1(TO) frequency as well as calculated value from the linear dependence reported in Ref.[22] for unstrained alloys. The z-axis lattice displacement ε_{zz} is plotted in the same graph, to present the correlation

between the out-of-plane lattice displacement and the measured A_1(TO) mode frequency. The large lattice distortion in z-axis for the 30% and 42% Al sample can be clearly seen from the deviation between the determined Raman value and the model.

C. Ellipsometry

Experimental and best-fit model spectra for AlN/Si and a selected $Al_xGa_{1-x}N$/AlN/Si sample are shown in Fig. IIIC1. In the mid-infrared spectra range, the ellipsometry data consists of interferences and phonon resonance features. The former one is sensitive to the structure of the thin film layers, and the latter one reflects about the composition ratios of the nitride alloys and assesses epilayer quality.

A pronounced "two-mode" behavior of the E_1(TO) mode is seen in the ellipsometry spectra. The energy, strength and broadening of the in-plane two modes were unambiguously determined through our ellipsometric model fitting. The RMSD generated from using our ellipsometric model is around 6.

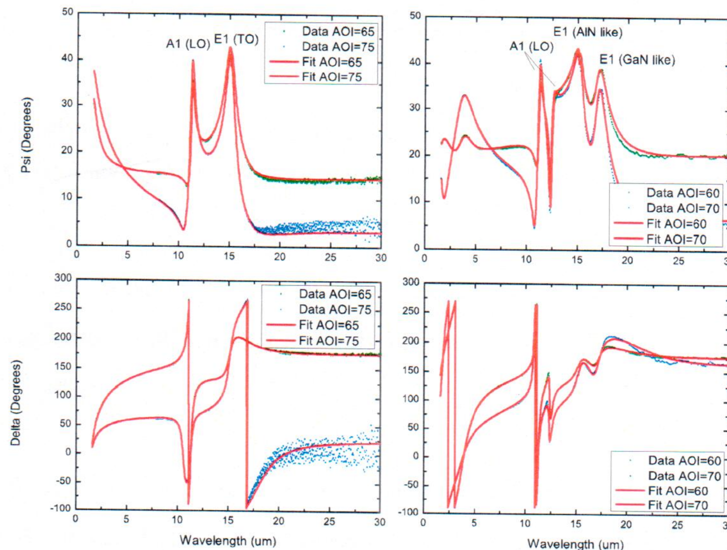

FIG. IIIC1 Measured and modeled ellipsometric angles Ψ and Δ. (Left panels) AlN/Si; (Right panels) $Al_{0.3}Ga_{0.7}N$/AlN/Si. The slight discrepancy between the model and experimental data at the long wavelength region, is due to the measurement artifact of the silicon backside reflection.

The retrieved infrared spectra of the in-plane "two-mode" transition are presented in Fig. IIIC2, in terms of the real part of the optical conductivity, which is defined as

$$\sigma_1 = \epsilon_0 \epsilon_2 \omega, \tag{8}$$

here ϵ_0 is the permittivity of vacuum, ϵ_2 is the imaginary part of the dielectric function, and ω is the frequency of the light wave.

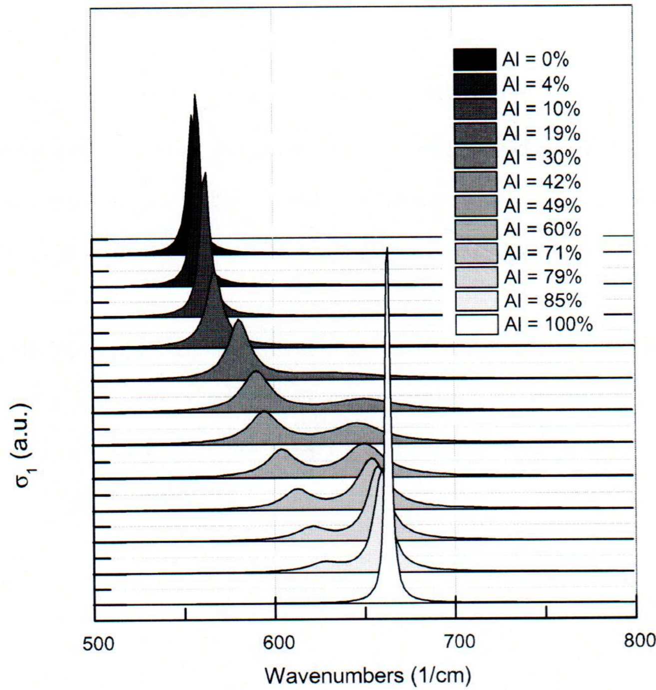

FIG. IIIC2 The optical conductivity derived from the ellipsometric measurement of the in-plane response. It clearly shows that the two peaks correspond to the two modes of E_1(TO) phonon, traditionally called GaN-like and AlN-like mode.

In Fig. IIIC2, the in-plane E_1(TO) phonon clearly shows the so-called "two-mode" behavior. The results are in a good agreement with the ab-initio calculation of the spectral density of states of the zone-center optical phonons in $Al_xGa_{1-x}N$ alloys [21].

The dependence of the so-called "loss function" with the Al composition is presented in Fig. IIIC3. Since the out-of-plane response consists of a single Lorentzian oscillator, the LO frequency is the position of the peak of the imaginary part of $\mathrm{Im}\{-1/\tilde{\epsilon}\}$; the A_1(LO) frequency corresponds to the zero crossing of the real part of dielectric function. The TO frequency has been fixed in our model, leaving only oscillator strength and damping to be fitted. The good agreement between the ellipsometric LO frequencies and the experimental values from Raman measurements can be seen in Fig. IIIC4.

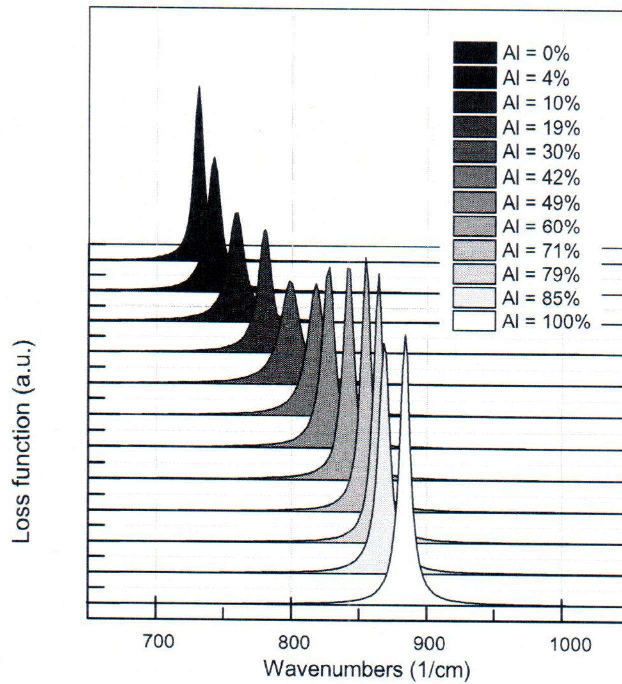

FIG. IIIC3 The dielectric loss function for the A_1 mode of the $Al_xGa_{1-x}N$ alloys. It is calculated from the out-of-plane dielectric function of the anisotropic ellipsometry model. The peak position corresponds to the LO frequency of the A_1 mode.

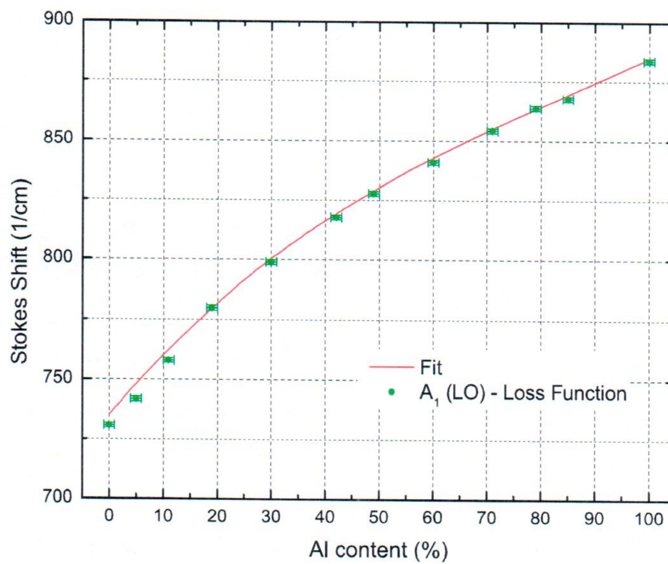

FIG. IIIC4 Compositional dependence of the A_1 (LO) mode frequency determined by ellipsometry. The calibration curve is identical to the one in the Fig. IIIB2.

The anisotropic nature of the nitride epilayers is also reflected in the electronic contribution of the permittivity, ϵ_∞. As shown in Fig. IIIC5, the out-of-plane best-fit values are consistently higher than the in-plane ones. Both components decrease with increasing Al content, due to the increase of the interband

electronic transition energies. These dependences are extracted using the parabolic fit in the Al range between 10% and 90%, giving

$$\epsilon_\infty(\text{out-of-plane}) = 5.58(3) - 0.005(1)x - 0.00008(2)x^2 \tag{9}$$

and

$$\epsilon_\infty(\text{in-plane}) = 5.20(1) - 0.0084(8)x - 0.000024(9)x^2, \tag{10}$$

where x is in atomic percent.

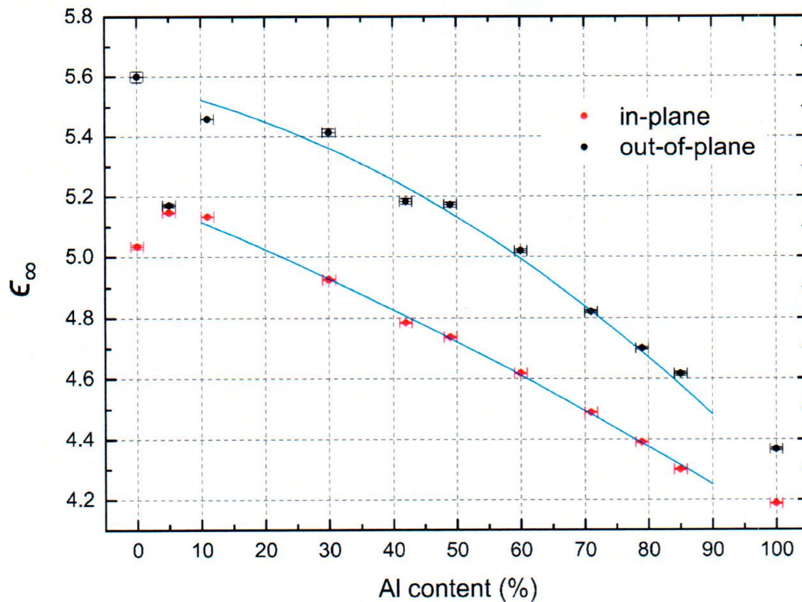

FIG. IIIC5 The electronic contribution to the dielectric function ϵ_∞ as a function of Al content. The blue solid lines present the parabolic fit in the Al range between 10% and 90%. The values obtained for 0% and 5% Al content samples are noticeably out of the trend, since the samples with low Al content are subject to structural defects due to the lattice mismatch.

IV. Conclusions

Combining XRD, Raman and mid-infrared ellipsometry, we have systematically studied a series of MOCVD grown $Al_xGa_{1-x}N$/AlN/Si samples. Using XRD, we have determined Al content with the accuracy of $\sim$ 1% and the anisotropic strain with the accuracy of 4×10^{-4}. Our $Al_xGa_{1-x}N$ epitaxial layers show a very small lattice deformation compared with the bulk material. The characteristic phonon mode frequencies were obtained using micro-Raman spectroscopy with excellent signal to noise ratio, using two scattering configurations. The uncertainty of the extracted phonon frequencies are below 0.5 cm^{-1}. Combining XRD and Raman results, we provide a calibration curve describing the relation between the A_1(LO) phonon mode energy and the Al content of the epitaxial nitride layer. The layer

thicknesses and the optically anisotropic response of the $Al_xGa_{1-x}N$ layers are obtained simultaneously from the analysis of the ellipsometry data. Good agreement between measured ellipsometric quantities Ψ and Δ and those calculated from our parametrized model has been achieved. The fit uses experimental values of the A_1(TO) determined by Raman experiment as *a-priori* knowledge, reducing systematic errors of our fitting procedure.

Acknowledgments

C.W. would like to acknowledge Adam Dubroka for the discussion of ellipsometry data and Dušan Hemzal for the guidance of Raman experiment. The authors would like to acknowledge financial support from the TH01011284 grant awarded by the Technology Agency of the Czech Republic.

References

[1] Shuji Nakamura, S. J. Pearton, and Gerhard Fasol. *The blue laser diode: the complete story*. Springer, Berlin ; New York, 2nd updated and extended ed edition, 2000.

[2] M. Asif Khan, J. N. Kuznia, J. M. Van Hove, N. Pan, and J. Carter. Observation of a two-dimensional electron gas in low pressure metalorganic chemical vapor deposited GaN-AlxGa1xN heterojunctions. *Applied Physics Letters*, 60(24):3027, 1992.

[3] F Scholz. Semipolar GaN grown on foreign substrates: a review. *Semiconductor Science and Technology*, 27(2):024002, February 2012.

[4] Yuan Lu, Xianglin Liu, Xiaohui Wang, Da-Cheng Lu, Dabing Li, Xiuxun Han, Guangwei Cong, and Zhanguo Wang. Influence of the growth temperature of the high-temperature AlN buffer on the properties of GaN grown on Si(111) substrate. *Journal of Crystal Growth*, 263(1-4):4–11, March 2004.

[5] W. V. Lundin, A. S. Usikov, A. V. Sakharov, V. V. Tretyakov, D. V. Poloskin, N. N. Ledentsov, and A. Hoffmann. Growth and Characterization of Thick Si-Doped AlGaN Epilayers on Sapphire Substrates. *physica status solidi (a)*, 176(1):379–384, November 1999.

[6] Min-Ho Kim, Young-Gu Do, Hyon Chol Kang, Do Young Noh, and Seong-Ju Park. Effects of step-graded Al[sub x]Ga[sub 1x]N interlayer on properties of GaN grown on Si(111) using ultrahigh vacuum chemical vapor deposition. *Applied Physics Letters*, 79(17):2713, 2001.

[7] A. V. Kuchuk, H. V. Stanchu, Chen Li, M. E. Ware, Yu. I. Mazur, V. P. Kladko, A. E. Belyaev, and G. J. Salamo. Measuring the depth profiles of strain/composition in AlGaN-graded layer by high-resolution x-ray diffraction. *Journal of Applied Physics*, 116(22):224302, December 2014.

[8] Chengyu He, Qiang Wu, Xizhang Wang, Yongliang Zhang, Lijun Yang, Ning Liu, Yu Zhao, Yinong Lu, and Zheng Hu. Growth and Characterization of Ternary AlGaN Alloy Nanocones across the Entire Composition Range. *ACS Nano*, 5(2):1291–1296, February 2011.

[9] H. Jiang, G. Y. Zhao, H. Ishikawa, T. Egawa, T. Jimbo, and M. Umeno. Determination of exciton transition energy and bowing parameter of AlGaN alloys in AlGaN/GaN heterostructure by means of reflectance measurement. *Journal of Applied Physics*, 89(2):1046, 2001.

[10] Z Dridi, B Bouhafs, and P Ruterana. First-principles investigation of lattice constants and bowing parameters in wurtzite Al $_x$ Ga $_{1\ x}$ N, In $_x$ Ga $_{1\ x}$ N and In $_x$ Al $_{1\ x}$ N alloys. *Semiconductor Science and Technology*, 18(9):850–856, September 2003.

[11] Laurie E. McNeil, Marcos Grimsditch, and Roger H. French. Vibrational Spectroscopy of Aluminum Nitride. *Journal of the American Ceramic Society*, 76(5):1132–1136, May 1993.

[12] A. Polian, M. Grimsditch, and I. Grzegory. Elastic constants of gallium nitride. *Journal of Applied Physics*, 79(6):3343, 1996.

[13] T. Prokofyeva, M. Seon, J. Vanbuskirk, M. Holtz, S. A. Nikishin, N. N. Faleev, H. Temkin, and S. Zollner. Vibrational properties of AlN grown on (111)-oriented silicon. *Physical Review B*, 63(12), March 2001.

[14] C. M. Herzinger, B. Johs, W. A. McGahan, J. A. Woollam, and W. Paulson. Ellipsometric determination of optical constants for silicon and thermally grown silicon dioxide via a multi-sample, multi-wavelength, multi-angle investigation. *Journal of Applied Physics*, 83(6):3323, 1998.

[15] D. A. G. Bruggeman. Berechnung verschiedener physikalischer Konstanten von heterogenen Substanzen. I. Dielektrizitätskonstanten und Leitfähigkeiten der Mischkörper aus isotropen Substanzen. *Annalen der Physik*, 416(7):636–664, 1935.

[16] J. Humlíček, R. Henn, and M. Cardona. Infrared vibrations in LaSrGaO 4 and LaSrAlO 4. *Physical Review B*, 61(21):14554–14563, June 2000.

[17] A. Kasic, M. Schubert, S. Einfeldt, D. Hommel, and T. E. Tiwald. Free-carrier and phonon properties of n - and p -type hexagonal GaN films measured by infrared ellipsometry. *Physical Review B*, 62(11):7365–7377, September 2000.

[18] S. Prakash, H. C. Gupta, and B. B. Tripathi. Two-mode behavior of mixed crystals. *Physical Review B*, 28(12):7390–7392, December 1983.

[19] Tista Basak, Mala N. Rao, and S.L. Chaplot. Study of one-mode, two-mode and three-mode phonon behavior in mixed zinc blende alloys. *Physica B: Condensed Matter*, 407(22):4478–4484, November 2012.

[20] P. Wisniewski, W. Knap, J. P. Malzac, J. Camassel, M. D. Bremser, R. F. Davis, and T. Suski. Investigation of optically active E[sub 1] transversal optic phonon modes in Al[sub x]Ga[sub 1x]N layers deposited on 6h–SiC substrates using infrared reflectance. *Applied Physics Letters*, 73(13):1760, 1998.

[21] Claudia Bungaro and Stefano de Gironcoli. Ab initio study of phonons in wurtzite Al[sub x]Ga[sub 1x]N alloys. *Applied Physics Letters*, 76(15):2101, 2000.

[22] V. Yu. Davydov, I. N. Goncharuk, A. N. Smirnov, A. E. Nikolaev, W. V. Lundin, A. S. Usikov, A. A. Klochikhin, J. Aderhold, J. Graul, O. Semchinova, and H. Harima. Composition dependence of optical phonon energies and Raman line broadening in hexagonal Al x Ga 1 x N alloys. *Physical Review B*, 65(12), March 2002.

[23] V. Darakchieva, B. Monemar, T. Paskova, S. Einfeldt, D. Hommel, and S. Lourdudoss. Phonons in strained AlGaN/GaN superlattices. *physica status solidi (c)*, 4(1):170–174, January 2007.